Characterization Method and Simple Design Formulas of MCS Lines Proposed for MMIC's

EIKICHI YAMASHITA, FELLOW, IEEE, KE REN LI, AND YOICHI SUZUKI

Abstract—**The proximity effects between microstrip lines and ground on monolithic microwave integrated circuits are estimated by using the rectangular boundary division method. The attenuation constant is calculated based on a new form of the incremental inductance rule. Micro-coplanar strip (MCS) lines are then proposed to avoid the proximity effects. Some results of structural design parameters of MCS lines are expressed in simple polynomial formulas for CAD.**

I. INTRODUCTION

THE RECENT development of monolithic microwave integrated circuits (MMIC's) is promising us many microwave circuit applications with small size, light weight, high reliability, and low cost. Small size allows the batch processing of hundreds of circuits per substrate wafer. It is therefore required that the exact design method or CAD of circuit patterns on substrate reduce chip area as small as possible to avoid tweaking.

Microstrip (MS) lines and coplanar waveguides (CPW) as shown in Fig. 1(a) and (b) have usually been used as interconnections between elements on high-dielectric-constant substrates such as GaAs. Pucel has pointed out the significance of "proximity effects" between the microstrip conductor and ground conductor on the top surface of the substrate in connection with circuit packing density in GaAs MMIC's, and the lack of any method to estimate the effects [1], [2].

It has also been pointed out that the lack of a ground plane on the top side surface of the microstrip structure is a considerable disadvantage when shunt element connections to the hot conductor are required. On the other hand, if CPW structures are employed, the loss of these structures would be larger than that of MS lines because of high current density near strip edges.

In this paper, the proximity effects are first estimated concerning transmission characteristics. In order to examine this structure, we extend an analysis method introduced in previous papers [3], [4]. The attenuation constant is calculated by expressing the incremental inductance rule in a new and simpler form. We propose, then, the use of "micro-coplanar strip lines" (MCS lines), which can easily be used for shunting elements, have the low-loss property of microstrip lines, and avoid the proximity effects, as the third choice of transmission lines for MMIC's. The structural design parameters of the micro-coplanar strip lines are expressed in simple polynomial formulas for CAD by a curve-fitting procedure.

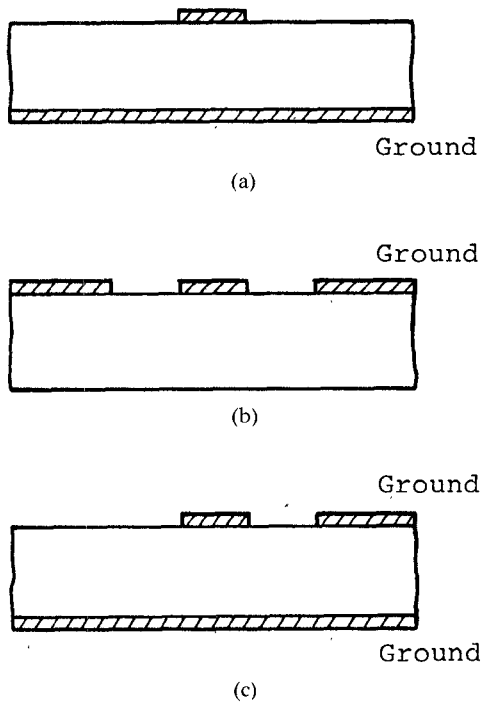

Fig. 1. Transmission lines for MMIC's. (a) MS lines. (b) CPW. (c) Illustration of proximity effects of MS lines, and also proposed MCS line structure.

II. RECTANGULAR BOUNDARY DIVISION METHOD

Two classes of the proximity effects defined by Pucel are the changes of transmission characteristics of MS lines in the vicinity of a ground plane and a chip edge, respectively [2]. The accurate estimation of the proximity effects in a structure of the first class as shown in Fig. 1(c) is now possible with the use of the analysis method described in this section.

Fig. 2 shows the dimensions and four divided regions with rectangular boundaries to analyze the above proximity effects. We essentially follow the same steps as the previous papers [3], [4] except for the setting of boundary

Manuscript received March 19, 1987; revised July 13, 1987.
The authors are with the University of Electro-Communications, Chofu-shi, Tokyo, Japan 182.
IEEE Log Number 8717109.

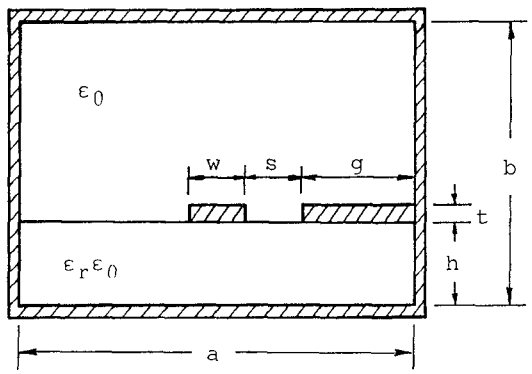

Fig. 2. The dimensions and four divided regions with rectangular boundaries of MCS lines for the analysis of the structure shown in Fig. 1(c).

conditions. For convenience, we would like to refer to this analysis method as the rectangular boundary division method.

Suppose that substrate thickness h and strip width w are small enough compared with wavelength in order to validate the quasi-TEM approximation. Scalar potentials as the solutions of Laplace's equation can be expanded in Fourier series in each rectangular boundary having two conductor side walls as follows:

$$\phi_1(x,y)=\sum_{n=1}^{\infty} A_{1n}\sinh(\xi_{1n}y)\sin(\xi_{1n}x) \tag{1a}$$

$$\phi_2(x,y)=\phi_{20}(x)+\sum_{n=1}^{\infty}\{A_{2n}\cosh[\xi_{2n}(y-h)]+B_{2n}\sinh[\xi_{2n}(y-h)]\}\sin(\xi_{2n}x) \tag{1b}$$

$$\phi_3(x,y)=\phi_{30}(x)+\sum_{n=1}^{\infty}\{A_{3n}\cosh[\xi_{3n}(y-h)]+B_{3n}\sinh[\xi_{3n}(y-h)]\}\cdot\sin[\xi_{3n}(x-d-w)] \tag{1c}$$

$$\phi_4(x,y)=\sum_{n=1}^{\infty} A_{4n}\sinh[\xi_{4n}(b-y)]\sin(\xi_{4n}x) \tag{1d}$$

where

$$\xi_{1n}=\frac{n\pi}{a}\qquad \xi_{2n}=\frac{n\pi}{d} \tag{2a}$$

$$\xi_{3n}=\frac{n\pi}{s}\qquad \xi_{4n}=\frac{n\pi}{a} \tag{2b}$$

$$\phi_{20}(x)=\frac{x}{d}\cdot V\qquad \phi_{30}(x)=\frac{d+w+s-x}{s}\cdot V \tag{2c}$$

and A_{1n}, A_{2n}, B_{2n}, A_{3n}, B_{3n}, and A_{4n} are unknown coefficients.

In the previous papers [3], [4], we imposed the continuation of potential functions as boundary conditions. In this paper, however, we impose the following continuation of the tangential components of electric fields as boundary conditions. The reason for this choice is the faster convergence of the Fourier series due to a physical relation that potentials are the integral of electric field functions:

$$\frac{\partial\phi_1(x,h)}{\partial x}=\frac{\partial\phi_2(x,h)}{\partial x}\qquad (0\le x\le d) \tag{3a}$$

$$\frac{\partial\phi_1(x,h)}{\partial x}=\frac{\partial\phi_3(x,h)}{\partial x}\qquad (d+w\le x\le d+w+s) \tag{3b}$$

$$\frac{\partial\phi_2(x,h+t)}{\partial x}=\frac{\partial\phi_4(x,h+t)}{\partial x}\qquad (0\le x\le d) \tag{3c}$$

$$\frac{\partial\phi_3(x,h+t)}{\partial x}=\frac{\partial\phi_4(x,h+t)}{\partial x}\qquad (d+w\le x\le d+w+s). \tag{3d}$$

Since ξ_{1n}, ξ_{2n}, ξ_{3n}, and ξ_{4n} are not identical, it is not possible to derive simple relations among the above unknown coefficients by solving equations obtained from the boundary conditions.

The other remaining boundary conditions, that is, the continuation of electric flux density, is equivalent to the minimization condition of the total electric field energy given by

$$U=\sum_{\nu=1}^{4}\frac{1}{2}\epsilon_\nu\iint_{S_\nu}\left\{\left(\frac{\partial\phi_\nu}{\partial x}\right)^2+\left(\frac{\partial\phi_\nu}{\partial y}\right)^2\right\}dx\,dy \tag{4}$$

where ϵ_ν and S_ν denote the dielectric permittivity and the cross-sectional area of the region ν ($\nu=1,2,3,4$). Exact potential solutions should minimize this total electric field energy.

When approximately minimizing U, the Rayleigh–Ritz procedure using A_{1n}, A_{2n}, B_{2n}, A_{3n}, B_{3n}, and A_{4n} can be considered. However, this procedure is numerically inefficient because of the infinite number of Fourier series coefficients. Instead, we use boundary tangential electric fields as trial functions.

Boundary tangential electric field functions are assumed in the following form:

$$E_\nu(x,h)=\begin{cases} f_1(x) & (0\le x\le d)\\ g_1(x) & (d+w\le x\le d+w+s)\\ 0 & \text{(elsewhere)}\end{cases} \tag{5a}$$

$$E_\nu(x,h+t)=\begin{cases} f_2(x) & (0\le x\le d)\\ g_2(x) & (d+w\le x\le d+w+s)\\ 0 & \text{(elsewhere)}.\end{cases} \tag{5b}$$

These are all unknown functions, but they can be related to the potential functions $\phi_\nu(x,y)$ ($\nu=1,2,3,4$) through the Fourier coefficients. An example is

$$E_\nu(x,h)=\sum_{n=1}^{\infty}-A_{1n}\xi_{1n}\sinh(\xi_{1n}h)\cos(\xi_{1n}x). \tag{6}$$

Therefore, A_{1n} is given by

$$A_{1n} = \frac{-2}{a\xi_{1n}\sinh(\xi_{1n}h)}\left\{\int_0^d f_1(x)\cos(\xi_{1n}x)\,dx + \int_{d+w}^{d+w+s} g_1(x)\cos(\xi_{1n}x)\,dx\right\}. \quad (7a)$$

In a similar fashion, other coefficients are related to boundary tangential electric field functions as

$$A_{2n} = -\frac{2}{d\xi_{2n}}\int_0^d f_1(x)\cos(\xi_{2n}x)\,dx \quad (7b)$$

$$B_{2n} = \frac{-2}{d\xi_{2n}\sinh(\xi_{2n}t)}\int_0^d f_2(x)\cos(\xi_{2n}x)\,dx + \frac{2}{d\xi_{2n}\tanh(\xi_{2n}t)}\int_0^d f_1(x)\cos(\xi_{2n}x)\,dx \quad (7c)$$

$$A_{3n} = -\frac{2}{s\xi_{3n}}\int_{d+w}^{d+w+s} g_1(x)\cos\xi_{3n}(x-d-w)]\,dx \quad (7d)$$

$$B_{3n} = \frac{-2}{s\xi_{3n}\sinh(\xi_{3n}t)}\cdot\int_{d+w}^{d+w+s} g_2(x)\cos[\xi_{3n}(x-d-w)]\,dx + \frac{2}{s\xi_{3n}\tanh(\xi_{3n}t)}\cdot\int_{d+w}^{d+w+s} g_1(x)\cos[\xi_{3n}(x-d-w)]\,dx \quad (7e)$$

$$A_{4n} = \frac{-2}{a\xi_{4n}\sinh[\xi_{4n}(b-h-t)]}\left\{\int_0^d f_2(x)\cos(\xi_{4n}x)\,dx + \int_{d+w}^{d+w+s} g_2(x)\cos(\xi_{4n}x)\,dx\right\}. \quad (7f)$$

Now the boundary electric field functions are expressed by spline functions as

$$f_1(x) = \sum_{i=0}^{m_1} p_{1i}F_i(x) \quad (8a)$$

$$f_2(x) = \sum_{i=0}^{m_1} p_{2i}F_i(x) \quad (8b)$$

$$g_1(x) = \sum_{j=0}^{m_2} q_{1j}G_j(x) \quad (8c)$$

$$g_2(x) = \sum_{j=0}^{m_2} q_{2j}G_j(x) \quad (8d)$$

where the spline functions are given as

$$F_i(x) = \begin{cases} (x_i - x_{i-1})^{-1}(x - x_{i-1}) & (x_{i-1} \leqslant x \leqslant x_i) \\ (x_{i+1} - x_i)^{-1}(x_{i+1} - x) & (x_i \leqslant x \leqslant x_{i+1}) \\ 0 & \text{(elsewhere)} \end{cases} \quad (9a)$$

$$G_j(x) = \begin{cases} (x_j - x_{j-1})^{-1}(x - x_{j-1}) & (x_{j-1} \leqslant x \leqslant x_j) \\ (x_{j+1} - x_j)^{-1}(x_{j+1} - x) & (x_j \leqslant x \leqslant x_{j+1}) \\ 0 & \text{(elsewhere)} \end{cases} \quad (9b)$$

and p_{li} and q_{lj} ($l = 1, 2$; $i = 0, 1, 2, \cdots, m_1$; $j = 0, 1, 2, \cdots, m_2$) are a finite n umber of newly introduced spline parameters which act as substitutes for an infinite number of Fourier coefficients: A_{1n}, A_{2n}, B_{2n}, A_{3n}, B_{3n}, and A_{4n}. The total electric field energy U can also be expressed by p_{li} and q_{lj}.

Because the strip conductor has the potential V, we have to impose four additional conditions on the boundary electric field functions as

$$H_1 = \int_0^d f_1(x)\,dx + V = 0 \quad (10a)$$

$$H_2 = \int_{d+w}^{d+w+s} g_1(x)\,dx - V = 0 \quad (10b)$$

$$H_3 = \int_0^d f_2(x)\,dx + V = 0 \quad (10c)$$

$$H_4 = \int_{d+w}^{d+w+s} g_2(x)\,dx - V = 0. \quad (10d)$$

Now, we define the functional of this variational problem as

$$J = \frac{1}{2}U + \sum_{k=1}^{4}\lambda_k H_k \quad (11)$$

in order to minimize the total energy under the above subsidiary conditions. The minimization conditions for this functional are

$$\frac{\partial J}{\partial p_{li}} = 0 \quad (12a)$$

$$\frac{\partial J}{\partial q_{lj}} = 0 \quad (12b)$$

$$\frac{\partial J}{\partial \lambda_k} = 0 \quad (12c)$$

($l = 1, 2$; $i = 0, 1, 2, \cdots, m_1$; $j = 0, 1, 2, \cdots, m_2$; $k = 1, 2, 3, 4$), which result in a set of linear simultaneous inhomogeneous equations of the spline parameters that can be solved on a computer (see the Appendix). The total energy U is calcu-

lated by substituting the solution of p_{li} and q_{lj} into the expressions of the Fourier coefficients, and then into the expression for U.

By equating the capacitance energy expression $CV^2/2$ and U, we obtain the line capacitance as

$$C = \frac{2U}{V^2}. \tag{13a}$$

When the dielectric materials are removed from the structure being considered, the line capacitance is similarly given by the total energy U_0 of that case

$$C_0 = \frac{2U_0}{V^2}. \tag{13b}$$

The characteristic impedance, effective dielectric constant, and wavelength reduction factor are consequently obtained, respectively, by

$$Z = \frac{1}{v_0\sqrt{CC_0}} \tag{14a}$$

$$\epsilon_{\text{eff}} = \frac{C}{C_0} \tag{14b}$$

$$\frac{\lambda}{\lambda_0} = \frac{1}{\sqrt{\epsilon_{\text{eff}}}} \tag{14c}$$

where v_0 is the light velocity in vacuum [3].

III. Attenuation Constants

A. Dielectric Attenuation Constant

When σ_{dv} is defined as the conductivity of the dielectric material in the region v, the dielectric attenuation constant is given by [5]

$$\alpha_d = \frac{\sum_v \sigma_{dv} \iint_{Sv} (\nabla\phi_v)^2 \, dx\, dy}{2v \sum_v \epsilon_v \iint_{Sv} (\nabla\phi_v)^2 \, dx\, dy} \tag{15a}$$

where v is the velocity of energy propagation. This expression can be rewritten as

$$\alpha_d = \frac{\pi}{\lambda} \cdot \sum_v \frac{U_v}{U} \tan\delta_v \qquad \text{(neper/unit length)} \tag{15b}$$

where U_v and $\tan\delta_v$ are the field energy and dielectric tangent in the region v, respectively.

B. Conductor Attenuation Constant

When σ_c is defined as the conductivity of the line conductor, the conductor surface resistance R_s at high frequencies is $(\omega\mu_0/2\sigma_c)^{1/2}$. Then, the conductor attenuation constant is given by [5]

$$\alpha_c = \frac{R_s \sum_v \int i_{Sv}^2 \, dl}{2v \sum_v \epsilon_v \iint_{Sv} (\nabla\phi_v)^2 \, dx\, dy} \tag{16a}$$

where i_{Sv} is the surface current density in the region v and the line integrals are carried out on all conductor surfaces. However, the calculation of α_c based on the above formula is complex and requires relatively long computation time. On the other hand, a formula called the incremental inductance rule for attenuation calculation was derived from the relation between the magnetic energy and line inductance [6] as

$$\alpha_c = \frac{R_s}{2\mu_0 Z} \sum_v \frac{\partial L}{\partial n_v} \tag{16b}$$

where μ_0 is the magnetic permeability in vacuum, $\partial/\partial n_v$ is the normal derivative to the conductor surface, and L is the line inductance.

In the TEM wave approximation, the line inductance of a nonmagnetic transmission line is the same as that of a line after removing dielectric materials. Therefore,

$$L = \frac{1}{v_0^2 C_0}. \tag{17}$$

At high frequencies, each conductor surface has a layer of skindepth

$$\delta_s = \left(\frac{2}{\omega\mu\sigma_c}\right)^{\frac{1}{2}} \tag{18}$$

and the line inductance is increased to L', which can be estimated only by decreasing the cross-sectional dimensions by half a skin depth from each surface [6]. The increase of the line inductance is then given by

$$\Delta L = L' - L = \frac{1}{v_0^2}\left(\frac{1}{C_0'} - \frac{1}{C_0}\right) \cong \sum_v \left(\frac{\partial L}{\partial n_v}\right)\frac{\delta_s}{2}. \tag{19}$$

Instead of the derivative formula (16b), therefore, we propose a difference formula for the simpler computation of α_c:

$$\alpha_c = \frac{\pi}{\lambda}\left(\frac{C_0}{C_0'} - 1\right) \qquad \text{(neper/unit length)}. \tag{20}$$

This formula is also preferred when the total field energy is estimated in the process of analysis. The ratio C_0/C_0' is a convenient form to cancel the errors of C_0 and C_0' due to the variational formulation and numerical computation.

IV. Proximity Effects and Micro-Coplanar Strip Lines

The rectangular boundary division method enables us to estimate the transmission characteristics, in particular, the conductor attenuation constant, of the thick-strip microstrip lines near ground plane on MMIC's.

Fig. 2 shows the four divided regions with rectangular boundaries to be analyzed. A large outer conductor box ($a \approx 100w$) is considered here for the purpose of analysis. Typical structural parameters in the case of GaAs MMIC's

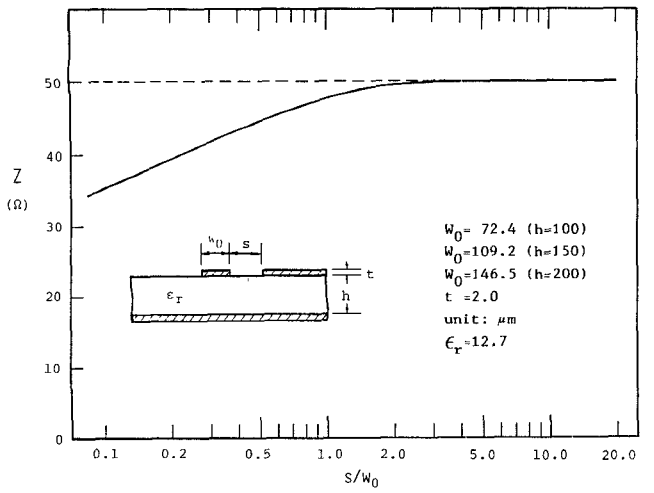

Fig. 3. The proximity effect on the characteristic impedance Z.

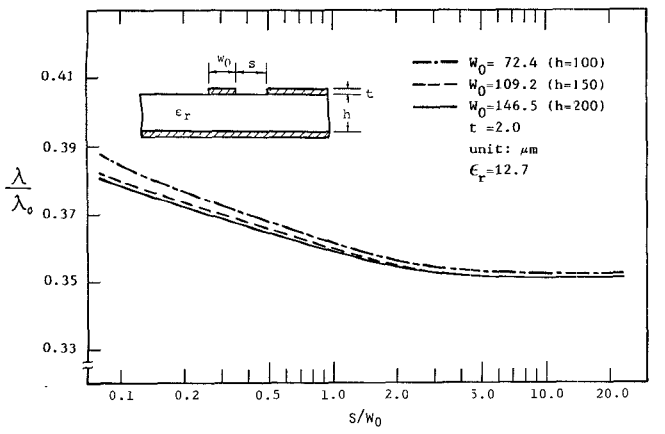

Fig. 4. The proximity effect on the ratio of guide wavelength to the free-space wavelength λ/λ_0.

are

$\epsilon_r = 12.7$ (GaAs)
$h = 100\ \mu$m, 150 μm, and 200 μm
$t = 1.5\ \mu$m, 2.0 μm
$\sigma_d = 10^{-7}$ S/cm (GaAs)
$\sigma_c = 4.17 \times 10^5$ S/cm (Au)
$f_0 = 10$ GHz.

The rapid change of electric fields at the strip conductor edge has to be considered in practice, and the number of spline knots must be large near the edges [3]. The quantities m_1 and m_2 are usually taken as 20, and 2/3 of them have to be located within a distance of $10w$ from a conductor edge.

Fig. 3 shows one of the proximity effects, that is, the expected decrease of the characteristic impedance of MS lines for decreasing separation s. Figs. 4 and 5 show the proximity effects on the guide wavelength and attenuation of MS lines, respectively.

As a natural consequence of establishing the analysis method for the proximity effects, we propose the third type of transmission lines for MMIC's, shown in Fig. 1(c), which we call micro-coplanar strip lines (MCS lines). A feature of MCS lines is to keep the characteristic impedance at a constant value by adjusting the strip width w against specified values of s. MCS lines can be designed by the rectangular boundary division method, can easily be used in shunting elements as CPW [7], have a low-loss property as MS lines, and can be transformed to either MS lines or CPW.

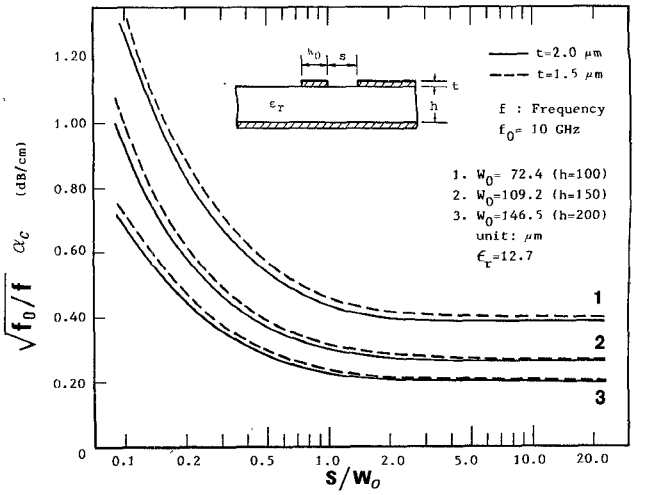

Fig. 5. The proximity effect on the conductor attenuation constant α_c.

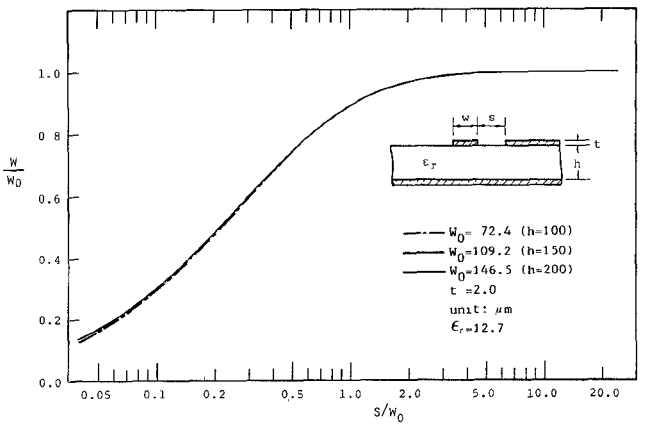

Fig. 6. The strip width w of 50-Ω MCS lines versus separation s.

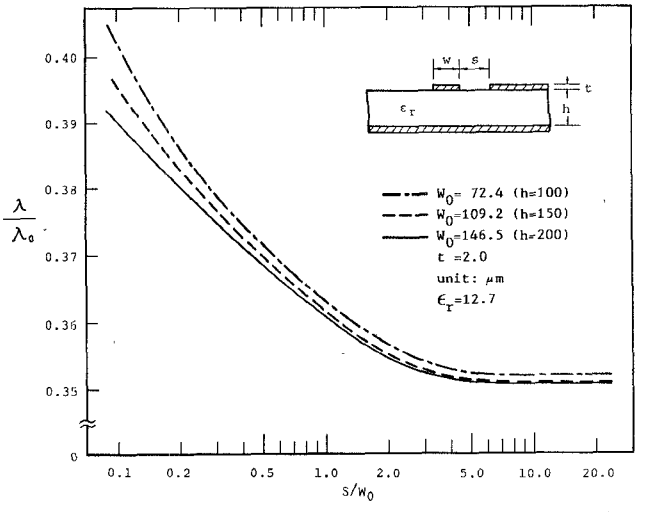

Fig. 7. The ratio of guide wavelength to free-space wavelength λ/λ_0 of 50-Ω MCS lines versus s.

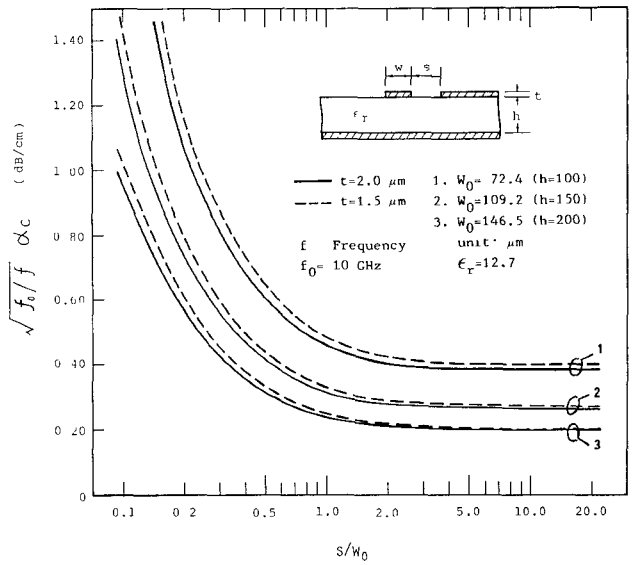

Fig. 8. The conductor attenuation constant α_c of 50-Ω MCS lines for gold as conductor material.

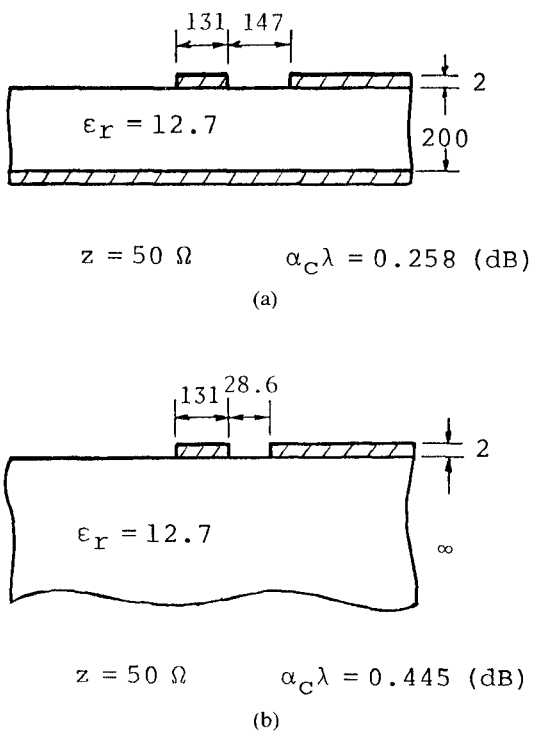

Fig. 9 Effects of ground plane on the attenuation constant of (a) MCS lines and (b) CPW with the same characteristic impedance.

Fig. 6 shows the designed strip width w of MCS lines for keeping the 50-Ω impedance against specified values of separation s. The quantity w_0 is the initially designed strip width for 50-Ω MS lines. Fig. 7 shows the ratio of guide wavelength to free-space wavelength λ/λ_0 of 50-Ω MCS lines against s. Fig. 8 shows the conductor attenuation constant of 50-Ω MCS lines at frequency f (GHz) using gold as the strip conductor material. Fig. 9 indicates the effects of a ground plane on the attenuation constant of MCS lines and CPW with the same characteristic impedance.

V. Approximate Polynomial Formulas

The above numerical relations can be expressed in simple approximate formulas by a curve-fitting procedure. The polynomial formula given below represents the designed strip width w of 50-Ω MCS lines in terms of separation s as shown in Fig. 6:

$$\frac{w}{w_0} = \eta_w \sum_{n=0}^{4} a_n u^n$$

where

$$u = \ln(s/w_0) \qquad (0.1 \leqslant s/w_0 \leqslant 10)$$

$$\eta_w = 1 - 0.28336((t/h) - 0.01)(1 - 3.6091u + 1.3875u^2)$$

$$a_0 = 0.89358 \qquad a_1 = 0.16458 \qquad a_2 = -0.72385 \times 10^{-1}$$

$$a_3 = -0.27323 \times 10^{-2} \qquad a_4 = 0.51618 \times 10^{-2}$$

$$72.4 \leqslant w_0 \leqslant 146.5 \qquad 100 \leqslant h \leqslant 200 \qquad \text{unit: } \mu\text{m}$$

$$0.01 \leqslant t/h \leqslant 0.02 \qquad \epsilon_r = 12.7 \qquad g > 10w_0.$$

A similar polynomial formula to express the guide wavelength shown in Fig. 7 has also been derived as follows:

$$\frac{\lambda}{\lambda_0} = \eta_\lambda \sum_{n=0}^{2} b_n u^n$$

where

$$\eta_\lambda = 1 + 0.66771((t/h) - 0.01) \cdot (1 - 0.79582u + 0.33722u^2)$$

$$b_0 = 0.36091 \qquad b_1 = -0.88745 \times 10^{-2}$$

$$b_2 = 0.17982 \times 10^{-2}$$

$$72.4 \leqslant w_0 \leqslant 146.5 \qquad 100 \leqslant h \leqslant 200 \qquad \text{unit: } \mu\text{m}$$

$$0.01 \leqslant t/h \leqslant 0.02 \qquad \epsilon_r = 12.7 \qquad g > 10w_0.$$

A discrepancy of about 1 percent has been recognized between values obtained from these approximate formulas and theoretical values derived from the above calculations for the strip width $w > (h/20)$. The theoretical values of the characteristic impedance and wavelength have errors of about 1 percent due to the nature of the variational method [3]. Though the experimental verification of MCS line parameters has not been given here, an extreme case of $s = \infty$ has been numerically checked with MS line parameters.

VI. Conclusions

It was shown in this paper that the rectangular boundary division method could be applied to estimate the proximity effects on the transmission characteristics of thick-strip MS lines on a high-dielectric-constant substrate such as GaAs, and to design structural parameters of newly proposed MCS lines. Part of MS lines can be easily transformed to MCS lines wherever the ground plane approaches the strip conductor. Some of numerical results were approximately expressed as polynomial formulas. A new form of the incremental inductance rule was introduced for the easier calculation of attenuation constant.

APPENDIX

For convenience, all unknown parameters are expressed in a unified fashion by the following vector:

$$\{x\} = \{x_0, x_1, \cdots x_m\} = \{p_{10}, \cdots, p_{1m1}, q_{10}, \cdots, q_{1m2}, p_{20}, \cdots, p_{2m1}, q_{20}, \cdots, q_{2m2}\}. \quad \text{(A1)}$$

When we define m as

$$m = 2m1 + 2m2 + 3$$

the energy given by (4) is rewritten as

$$U = \frac{1}{2}\epsilon_0\left(\frac{t}{d} + \frac{t}{s}\right)V^2 + \sum_{i=0}^{m}\sum_{j=0}^{m} K_{ij}x_i x_j \quad \text{(A2)}$$

where

$$K_{ij} = K_{1ij} + K_{2ij} + K_{3ij} + K_{4ij}$$

$$K_{ji} = K_{ij}$$

$$K_{1ij} = \begin{cases} \sum_{n=1}^{\infty} H_{1n} I_{1ni} I_{1nj} & (0 \leqslant i, j \leqslant M1) \\ \sum_{n=1}^{\infty} H_{1n} I_{1ni} I'_{1nj} & (0 \leqslant i \leqslant M1, \; M1+1 \leqslant j \leqslant M2) \\ \sum_{n=1}^{\infty} H_{1n} I'_{1ni} I'_{1nj} & (M1+1 \leqslant i, j \leqslant M2) \\ 0 & \text{(elsewhere)} \end{cases}$$

$$K_{2ij} = \begin{cases} \sum_{n=1}^{\infty} H_{2n} I_{2ni} I_{2nj} & (0 \leqslant i, j \leqslant M1) \\ \sum_{n=1}^{\infty} -H'_{2n} I_{2ni} I_{2nj} & (0 \leqslant i \leqslant M1, \; M2+1 \leqslant j \leqslant M3) \\ \sum_{n=1}^{\infty} H_{2n} I_{2ni} I_{2nj} & (M2+1 \leqslant i, j \leqslant M3) \\ 0 & \text{(elsewhere)} \end{cases}$$

$$K_{3ij} = \begin{cases} \sum_{n=1}^{\infty} H_{3n} I_{3ni} I_{3nj} & (M1+1 \leqslant i, j \leqslant M2) \\ \sum_{n=1}^{\infty} -H'_{3n} I_{3ni} I_{3nj} & (M1+1 \leqslant i \leqslant M2, \; M3+1 \leqslant j \leqslant M4) \\ \sum_{n=1}^{\infty} H_{3n} I_{3ni} I_{3nj} & (M3+1 \leqslant i, j \leqslant M4) \\ 0 & \text{(elsewhere)} \end{cases}$$

$$K_{4ij} = \begin{cases} \sum_{n=1}^{\infty} H_{4n} I_{4ni} I_{4nj} & (M2+1 \leqslant i, j \leqslant M3) \\ \sum_{n=1}^{\infty} H_{4n} I_{4ni} I'_{4nj} & (M2+1 \leqslant i \leqslant M3, \; M3+1 \leqslant j \leqslant M4) \\ \sum_{n=1}^{\infty} H_{4n} I'_{4ni} I'_{4nj} & (M3+1 \leqslant i, j \leqslant M4) \\ 0 & \text{(elsewhere)} \end{cases}$$

$$M1 = m1 \qquad M2 = m1 + m2 + 1$$

$$M3 = 2m1 + m2 + 2 \qquad M4 = m$$

$$I_{1ni} = \frac{1}{\xi_{1n}^2}\left(\frac{\cos\xi_{1n}x_i^{(1)} - \cos\xi_{1n}x_{i-1}^{(1)}}{x_i^{(1)} - x_{i-1}^{(1)}} + \frac{\cos\xi_{1n}x_i^{(1)} - \cos\xi_{1n}x_{i+1}^{(1)}}{x_{i+1}^{(1)} - x_i^{(1)}}\right)$$

$$I'_{1ni} = \frac{1}{\xi_{1n}^2}\left(\frac{\cos\xi_{1n}x_i^{(2)} - \cos\xi_{1n}x_{i-1}^{(2)}}{x_i^{(2)} - x_{i-1}^{(2)}} + \frac{\cos\xi_{1n}x_i^{(2)} - \cos\xi_{1n}x_{i+1}^{(2)}}{x_{i+1}^{(2)} - x_i^{(2)}}\right)$$

$$I_{2ni} = \frac{1}{\xi_{2n}^2}\left(\frac{\cos\xi_{2n}x_i^{(1)} - \cos\xi_{2n}x_{i-1}^{(1)}}{x_i^{(1)} - x_{i-1}^{(1)}} + \frac{\cos\xi_{2n}x_i^{(1)} - \cos\xi_{2n}x_{i+1}^{(1)}}{x_{i+1}^{(1)} - x_i^{(1)}}\right)$$

$$I_{3ni} = \frac{1}{\xi_{3n}^2}\left(\frac{\cos\xi_{3n}x_i^{(2)} - \cos\xi_{3n}x_{i-1}^{(2)}}{x_i^{(2)} - x_{i-1}^{(2)}} + \frac{\cos\xi_{3n}x_i^{(2)} - \cos\xi_{3n}x_{i+1}^{(2)}}{x_{i+1}^{(2)} - x_i^{(2)}}\right)$$

$$I_{4ni} = \frac{1}{\xi_{4n}^2}\left(\frac{\cos\xi_{4n}x_i^{(1)} - \cos\xi_{4n}x_{i-1}^{(1)}}{x_i^{(1)} - x_{i-1}^{(1)}} + \frac{\cos\xi_{4n}x_i^{(1)} - \cos\xi_{4n}x_{i+1}^{(1)}}{x_{i+1}^{(1)} - x_i^{(1)}}\right)$$

$$I'_{4ni} = \frac{1}{\xi_{4n}^2}\left(\frac{\cos\xi_{4n}x_i^{(2)} - \cos\xi_{4n}x_{i-1}^{(2)}}{x_i^{(2)} - x_{i-1}^{(2)}} + \frac{\cos\xi_{4n}x_i^{(2)} - \cos\xi_{4n}x_{i+1}^{(2)}}{x_{i+1}^{(2)} - x_i^{(2)}}\right)$$

$$0 \leqslant x_i^{(1)} \leqslant d \qquad (i = 0, \cdots, m1)$$

$$d + w \leqslant x_i^{(2)} \leqslant d + w + s \qquad (i = 0, \cdots, m2)$$

$$H_{1n} = \frac{\epsilon_1}{n\pi\tanh(\xi_{1n}h)}$$

$$H_{2n} = \frac{\epsilon_2}{n\pi\tanh(\xi_{2n}t)} \qquad H'_{2n} = \frac{\epsilon_2}{n\pi\sinh(\xi_{2n}t)}$$

$$H_{3n} = \frac{\epsilon_3}{n\pi\tanh(\xi_{3n}t)} \qquad H'_{3n} = \frac{\epsilon_3}{n\pi\sinh(\xi_{3n}t)}$$

$$H_{4n} = \frac{\epsilon_4}{n\pi\tanh(\xi_{4n}(b-h-t))}.$$

The subsidiary conditions given by (9) and (10) can be rewritten as

$$\left.\begin{aligned} \sum_{i=0}^{m1}\delta_i^{(1)}p_{1i} &= -V & \sum_{i=0}^{m1}\delta_i^{(1)}p_{2i} &= -V \\ \sum_{j=0}^{m2}\delta_j^{(2)}q_{1j} &= V & \sum_{j=0}^{m2}\delta_j^{(2)}q_{2j} &= V \end{aligned}\right\} \quad \text{(A3)}$$

where

$$\delta_i^{(1)} = \frac{1}{2}\left(x_{i+1}^{(1)} - x_{i-1}^{(1)}\right) \qquad (i = 1, \cdots, m1-1)$$

$$\delta_0^{(1)} = \frac{1}{2}\left(x_1^{(1)} - x_0^{(1)}\right) \qquad \delta_{m1}^{(1)} = \frac{1}{2}\left(x_{m1}^{(1)} - x_{m1-1}^{(1)}\right)$$

$$\delta_j^{(2)} = \frac{1}{2}\left(x_{j+1}^{(2)} - x_{j-1}^{(2)}\right) \qquad (j = 1, \cdots, m2-1)$$

$$\delta_0^{(2)} = \frac{1}{2}\left(x_1^{(2)} - x_0^{(2)}\right) \qquad \delta_{m2}^{(2)} = \frac{1}{2}\left(x_{m2}^{(2)} - x_{m2-1}^{(2)}\right).$$

Finally, a set of linear, simultaneous, inhomogeneous equations to be solved on a computer is given by

$$\left.\begin{aligned}
\sum_{j=0}^{m} K_{ij}x_j + \lambda x_j &= 0 \qquad (i=0,\cdots,m)\\
\sum_{j=0}^{m1} \delta_j^{(1)} x_j &= -V\\
\sum_{j=0}^{m2} \delta_j^{(2)} x_{j+M1+1} &= V\\
\sum_{j=0}^{m1} \delta_j^{(1)} x_{j+M2+1} &= -V\\
\sum_{j=0}^{m2} \delta_j^{(2)} x_{j+M3+1} &= V
\end{aligned}\right\} \quad \text{(A4)}$$

where

$$\lambda = \begin{cases} \lambda_1, & 0 \leqslant i \leqslant M1 \\ \lambda_2, & M1+1 \leqslant i \leqslant M2 \\ \lambda_3, & M2+1 \leqslant i \leqslant M3 \\ \lambda_4, & M3+1 \leqslant i \leqslant M4. \end{cases}$$

ACKNOWLEDGMENT

The authors thank Dr. K. Atsuki of the University of Electro-Communications and K. Mishima and Ms. E. Kaneko of Toshiba Corporation for their helpful comments and assistance.

REFERENCES

[1] R. A. Pucel, "Design consideration for monolithic microwave circuits," *IEEE Trans. Microwave Theory Tech.*, vol. MTT-29, pp. 513–534, June 1981.

[2] R. A. Pucel, "MMIC's modelling and CAD—Where do we go from here?" in *Proc. 16th European Microwave Conf.*, Sept. 1986, pp. 61–70.

[3] E. Yamashita, B. Y. Wang, K. Atsuki, and K. R. Li, "Effects of side-wall grooves on transmission characteristics of suspended striplines," *IEEE Trans. Microwave Theory Tech.*, vol. MTT-33, pp. 1323–1328, Dec. 1985.

[4] E. Yamashita, M. Nakajima, and K. Atsuki, "Analysis method for generalized suspended striplines," *IEEE Trans. Microwave Theory Tech.*, vol. MTT-34, pp. 1457–1463, Dec. 1986.

[5] E. Yamashita and K. Atsuki, "Strip line with rectangular outer conductor and three dielectric layers," *IEEE Trans. Microwave Theory Tech.*, vol. MTT-18, pp. 238–244, May 1970.

[6] R. A. Pucel, D. J. Masse, and C. P. Hartwig, "Losses in microstrip," *IEEE Trans. Microwave Theory Tech.*, vol. MTT-16, pp. 342–350, June 1968.

[7] C. P. Wen, "Coplanar-waveguide directional couplers," *IEEE Trans. Microwave Theory Tech.*, vol. MTT-18, pp. 318–322, June 1970.

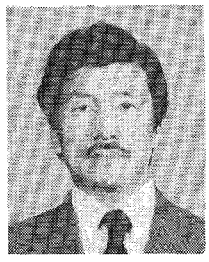

Eikichi Yamashita (M'66–SM'79–F'84) was born in Tokyo, Japan, on February 4, 1933. He received the B.S. degree from the University of Electro-Communications, Tokyo, and the M.S. and Ph.D. degrees from the University of Illinois, Urbana, all in electrical engineering, in 1956, 1963, and 1966, respectively.

From 1956 to 1964, he was a member of the Research Staff on millimeter-wave engineering at the Electrotechnical Laboratory, Tokyo. While on leave from 1961 to 1963 and from 1964 to 1966, he studied solid-state devices in the millimeter-wave region at the Electro-Physics Laboratory, University of Illinois. From 1966 to 1967, he was with the Antenna Laboratory, University of Illinois. He was named Associate Professor in 1967 and Professor in 1977 in the Department of Applied Electronics, the University of Electro-Communications, Tokyo. His research work since 1956 has been on microstrip transmission lines, suspended strip lines, wave propagation in gaseous plasma, pyroelectric-effect detectors in the submillimeter-wave region, tunnel-diode oscillators, wide-band laser modulators, and various types of optical fibers.

Dr. Yamashita is a member of the Institute of Electronics, Information and Communication Engineers of Japan and Sigma Xi. During the period 1980–1984, he served as Associated Editor of the IEEE TRANSACTIONS ON MICROWAVE THEORY AND TECHNIQUES. He was elected Chairman of the Tokyo Chapter of the MTT Society for the period 1985–1986.

✠

Ke Ren Li was born in Jiang Su, China, on January 22, 1962. He received the B.S. degree from the Nanjing Institute of Technology, China, in July 1983, and the M.E. degree from the University of Electro-Communications, Japan, in March 1987.

He is currently studying at the University of Tokyo, Japan, for the Ph.D. degree. His research interests include the computer-aided analysis and design of microwave and optical wave circuits.

✠

Yoichi Suzuki was born in Otaru, Japan, on May 9, 1950. He received the B.S., M.S., and Dr. Eng. degrees from Hokkaido University, Sapporo, all in electrical engineering, in 1973, 1975, and 1979, respectively.

He was named Research Assistant in 1980 and Instructor in 1987 in the Department of Electronics, the University of Electro-Communications, Tokyo, Japan. His research interests are in computer holography, millimeter-wave holography, and optical fiber gyroscope.

Dr. Suzuki is a member of the Institute of Electronics, Information and Communication Engineers of Japan and the Japan Society of Applied Physics.